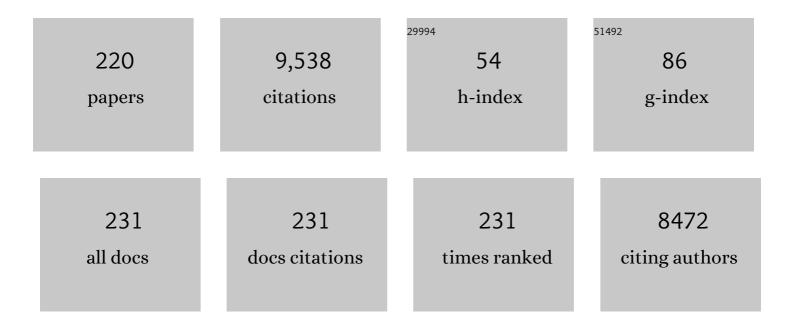
List of Publications by Year in descending order

Source: https://exaly.com/author-pdf/7950085/publications.pdf Version: 2024-02-01



#	Article	IF	CITATIONS
1	Drug–target residence time: critical information for lead optimization. Current Opinion in Chemical Biology, 2010, 14, 467-474.	2.8	391
2	The isoniazid-NAD adduct is a slow, tight-binding inhibitor of InhA, the Mycobacterium tuberculosis enoyl reductase: Adduct affinity and drug resistance. Proceedings of the National Academy of Sciences of the United States of America, 2003, 100, 13881-13886.	3.3	298
3	Drug Discovery Using Chemical Systems Biology: Repositioning the Safe Medicine Comtan to Treat Multi-Drug and Extensively Drug Resistant Tuberculosis. PLoS Computational Biology, 2009, 5, e1000423.	1.5	283
4	Inhibitors of Fabl, an Enzyme Drug Target in the Bacterial Fatty Acid Biosynthesis Pathway. Accounts of Chemical Research, 2008, 41, 11-20.	7.6	246
5	High Affinity InhA Inhibitors with Activity against Drug-Resistant Strains of Mycobacterium tuberculosis. ACS Chemical Biology, 2006, 1, 43-53.	1.6	234
6	Inhibition of InhA, the Enoyl Reductase fromMycobacterium tuberculosis, by Triclosan and Isoniazidâ€. Biochemistry, 2000, 39, 7645-7650.	1.2	226
7	Structural basis and mechanism of enoyl reductase inhibition by triclosan. Journal of Molecular Biology, 1999, 290, 859-865.	2.0	201
8	Observation of Excited-State Proton Transfer in Green Fluorescent Protein using Ultrafast Vibrational Spectroscopy. Journal of the American Chemical Society, 2005, 127, 2864-2865.	6.6	189
9	Drug–Target Kinetics in Drug Discovery. ACS Chemical Neuroscience, 2018, 9, 29-39.	1.7	189
10	A Machine Learning-Based Method To Improve Docking Scoring Functions and Its Application to Drug Repurposing. Journal of Chemical Information and Modeling, 2011, 51, 408-419.	2.5	175
11	Probing the Ground State Structure of the Green Fluorescent Protein Chromophore Using Raman Spectroscopyâ€. Biochemistry, 2000, 39, 4423-4431.	1.2	161
12	A Slow, Tight Binding Inhibitor of InhA, the Enoyl-Acyl Carrier Protein Reductase from Mycobacterium tuberculosis. Journal of Biological Chemistry, 2010, 285, 14330-14337.	1.6	155
13	Novel Trisubstituted Benzimidazoles, Targeting <i>Mtb</i> FtsZ, as a New Class of Antitubercular Agents. Journal of Medicinal Chemistry, 2011, 54, 374-381.	2.9	145
14	Marine natural products from the Turkish sponge Agelas oroides that inhibit the enoyl reductases from Plasmodium falciparum, Mycobacterium tuberculosis and Escherichia coli. Bioorganic and Medicinal Chemistry, 2007, 15, 6834-6845.	1.4	129
15	Translating slow-binding inhibition kinetics into cellular and in vivo effects. Nature Chemical Biology, 2015, 11, 416-423.	3.9	127
16	Roles of Tyrosine 158 and Lysine 165 in the Catalytic Mechanism of InhA, the Enoyl-ACP Reductase fromMycobacterium tuberculosisâ€. Biochemistry, 1999, 38, 13623-13634.	1.2	117
17	Ultrafast Structural Dynamics in BLUF Domains:  Transient Infrared Spectroscopy of AppA and Its Mutants. Journal of the American Chemical Society, 2007, 129, 15556-15564.	6.6	113
18	An Alternate Proton Acceptor for Excited-State Proton Transfer in Green Fluorescent Protein: Rewiring GFP. Journal of the American Chemical Society, 2008, 130, 1227-1235.	6.6	108

#	Article	IF	CITATIONS
19	Isotopic Labeling and Normal-Mode Analysis of a Model Green Fluorescent Protein Chromophore. Journal of Physical Chemistry B, 2002, 106, 6056-6066.	1.2	107
20	Slow-Onset Inhibition of the Fabl Enoyl Reductase from <i>Francisella tularensis</i> : Residence Time and <i>in Vivo</i> Activity. ACS Chemical Biology, 2009, 4, 221-231.	1.6	106
21	Structureâ^'Activity Studies of the Inhibition of FabI, the Enoyl Reductase from Escherichia coli, by Triclosan:  Kinetic Analysis of Mutant FabIs. Biochemistry, 2003, 42, 4406-4413.	1.2	105
22	Inhibition of the Bacterial Enoyl Reductase Fabl by Triclosan:Â A Structureâ^'Reactivity Analysis of Fabl Inhibition by Triclosan Analoguesâ€. Journal of Medicinal Chemistry, 2004, 47, 509-518.	2.9	101
23	Structure of Acyl Carrier Protein Bound to Fabl, the FASII Enoyl Reductase from Escherichia coli. Journal of Biological Chemistry, 2006, 281, 39285-39293.	1.6	101
24	Targeting FtsZ for Antituberculosis Drug Discovery:Â Noncytotoxic Taxanes as Novel Antituberculosis Agents. Journal of Medicinal Chemistry, 2006, 49, 463-466.	2.9	100
25	Light-Driven Decarboxylation of Wild-Type Green Fluorescent Proteinâ€. Journal of the American Chemical Society, 2003, 125, 6919-6926.	6.6	99
26	Direct inhibitors of InhA are active against <i>Mycobacterium tuberculosis</i> . Science Translational Medicine, 2015, 7, 269ra3.	5.8	98
27	Ultrafast Excited and Ground-State Dynamics of the Green Fluorescent Protein Chromophore in Solution. Journal of Physical Chemistry A, 2004, 108, 4587-4598.	1.1	97
28	Synthesis and SAR studies of 1,4-benzoxazine MenB inhibitors: Novel antibacterial agents against Mycobacterium tuberculosis. Bioorganic and Medicinal Chemistry Letters, 2010, 20, 6306-6309.	1.0	89
29	Crystal Structure of Mycobacterium tuberculosis MenB, a Key Enzyme in Vitamin K2 Biosynthesis. Journal of Biological Chemistry, 2003, 278, 42352-42360.	1.6	86
30	Discovery of anti-TB agents that target the cell-division protein FtsZ. Future Medicinal Chemistry, 2010, 2, 1305-1323.	1.1	79
31	Synthesis and Spectroscopic Studies of Model Red Fluorescent Protein Chromophores. Organic Letters, 2002, 4, 1523-1526.	2.4	78
32	Staphylococcus aureus Fabl: Inhibition, Substrate Recognition, and Potential Implications for InÂVivo Essentiality. Structure, 2012, 20, 802-813.	1.6	78
33	Targeting InhA, the FASII Enoyl-ACP Reductase: SAR Studies on Novel Inhibitor Scaffolds. Current Topics in Medicinal Chemistry, 2012, 12, 672-693.	1.0	76
34	Synthesis and in vitro antimycobacterial activity of B-ring modified diaryl ether InhA inhibitors. Bioorganic and Medicinal Chemistry Letters, 2008, 18, 3029-3033.	1.0	75
35	Ground state isomerization of a model green fluorescent protein chromophore. FEBS Letters, 2003, 549, 35-38.	1.3	74
36	Proton Relay Reaction in Green Fluorescent Protein (GFP):Â Polarization-Resolved Ultrafast Vibrational Spectroscopy of Isotopically Edited GFP. Journal of Physical Chemistry B, 2006, 110, 22009-22018.	1.2	73

#	Article	IF	CITATIONS
37	Mechanism-based inhibitors of MenE, an acyl-CoA synthetase involved in bacterial menaquinone biosynthesis. Bioorganic and Medicinal Chemistry Letters, 2008, 18, 5963-5966.	1.0	73
38	Forces, bond lengths, and reactivity: fundamental insight into the mechanism of enzyme catalysis. Biochemistry, 1992, 31, 9122-9125.	1.2	71
39	Crystal Structures of Mycobacterium tuberculosis KasA Show Mode of Action within Cell Wall Biosynthesis and its Inhibition by Thiolactomycin. Structure, 2009, 17, 1004-1013.	1.6	66
40	Radiosynthesis and Bioimaging of the Tuberculosis Chemotherapeutics Isoniazid, Rifampicin and Pyrazinamide in Baboons. Journal of Medicinal Chemistry, 2010, 53, 2882-2891.	2.9	66
41	FtsZ: A Novel Target for Tuberculosis Drug Discovery. Current Topics in Medicinal Chemistry, 2007, 7, 527-543.	1.0	65
42	Proteins in Action: Femtosecond to Millisecond Structural Dynamics of a Photoactive Flavoprotein. Journal of the American Chemical Society, 2013, 135, 16168-16174.	6.6	65
43	A Structural and Energetic Model for the Slow-Onset Inhibition of the <i>Mycobacterium tuberculosis</i> Enoyl-ACP Reductase InhA. ACS Chemical Biology, 2014, 9, 986-993.	1.6	63
44	Rational Design of Broad Spectrum Antibacterial Activity Based on a Clinically Relevant Enoyl-Acyl Carrier Protein (ACP) Reductase Inhibitor. Journal of Biological Chemistry, 2014, 289, 15987-16005.	1.6	63
45	Positron Emission Tomography Imaging with 2-[ <sup>18</sup> F]F- <i>p</i> -Aminobenzoic Acid Detects <i>Staphylococcus aureus</i> Infections and Monitors Drug Response. ACS Infectious Diseases, 2018, 4, 1635-1644.	1.8	63
46	Structure and Mechanism of Mbtl, the Salicylate Synthase from Mycobacterium tuberculosis. Biochemistry, 2007, 46, 954-964.	1.2	62
47	Mechanism of the Intramolecular Claisen Condensation Reaction Catalyzed by MenB, a Crotonase Superfamily Member. Biochemistry, 2011, 50, 9532-9544.	1.2	62
48	Role of Glutamate 144 and Glutamate 164 in the Catalytic Mechanism of Enoyl-CoA Hydrataseâ€. Biochemistry, 1999, 38, 9508-9516.	1.2	61
49	Ultrafast Vibrational Spectroscopy of the Flavin Chromophore. Journal of Physical Chemistry B, 2006, 110, 20107-20110.	1.2	61
50	Mechanism and Inhibition of saFabI, the Enoyl Reductase from <i>Staphylococcus aureus</i> . Biochemistry, 2008, 47, 4228-4236.	1.2	61
51	Noninvasive Determination of 2-[ <sup>18</sup> F]-Fluoroisonicotinic Acid Hydrazide Pharmacokinetics by Positron Emission Tomography in Mycobacterium tuberculosis-Infected Mice. Antimicrobial Agents and Chemotherapy, 2012, 56, 6284-6290.	1.4	60
52	Enoyl-Coenzyme A Hydratase-Catalyzed Exchange of the .alphaProtons of Coenzyme A Thiol Esters: A Model for an Enolized Intermediate in the Enzyme-Catalyzed Elimination?. Biochemistry, 1994, 33, 14733-14742.	1.2	59
53	Excited state dynamics in the green fluorescent protein. Journal of Photochemistry and Photobiology A: Chemistry, 2009, 205, 1-11.	2.0	59
54	Rational Optimization of Drug-Target Residence Time: Insights from Inhibitor Binding to the <i>Staphylococcus aureus</i> Fabl Enzyme–Product Complex. Biochemistry, 2013, 52, 4217-4228.	1.2	58

#	Article	IF	CITATIONS
55	Electronic Rearrangement Induced by Substrate Analog Binding to the Enoyl-CoA Hydratase Active Site: Evidence for Substrate Activation. Biochemistry, 1994, 33, 12635-12643.	1.2	56
56	H-Bonding in Alcohols Is Reflected in the Cαâ^'H Bond Strength:  Variation of Câ^'D Vibrational Frequency and Fractionation Factor. Journal of the American Chemical Society, 2000, 122, 11660-11669.	6.6	56
57	Targeting Fatty Acid Biosynthesis for the Development of Novel Chemotherapeutics against <i>Mycobacterium tuberculosis</i> : Evaluation of A-Ring-Modified Diphenyl Ethers as High-Affinity InhA Inhibitors. Antimicrobial Agents and Chemotherapy, 2007, 51, 3562-3567.	1.4	54
58	Fourier-transform infra-red studies of the alkaline isomerization of mitochondrial cytochrome c and the ionization of carboxylic acids. Biochemical Journal, 1989, 258, 599-605.	1.7	53
59	Lysine 190 Is the Catalytic Base in MenF, the Menaquinone-Specific Isochorismate Synthase from Escherichia coli:  Implications for an Enzyme Family. Biochemistry, 2007, 46, 946-953.	1.2	53
60	Length of the acyl carbonyl bond in acyl-serine proteases correlates with reactivity. Biochemistry, 1990, 29, 10723-10727.	1.2	51
61	Unlocking the Secrets of Enzyme Power Using Raman Spectroscopy. Accounts of Chemical Research, 1995, 28, 8-13.	7.6	51
62	Photoexcitation of the Blue Light Using FAD Photoreceptor AppA Results in Ultrafast Changes to the Protein Matrix. Journal of the American Chemical Society, 2011, 133, 16893-16900.	6.6	51
63	Stable Analogues of OSBâ€AMP: Potent Inhibitors of MenE, the <i>o</i> â€Succinylbenzoateâ€CoA Synthetase from Bacterial Menaquinone Biosynthesis. ChemBioChem, 2012, 13, 129-136.	1.3	51
64	Structural Basis for the Recognition of Mycolic Acid Precursors by KasA, a Condensing Enzyme and Drug Target from Mycobacterium Tuberculosis. Journal of Biological Chemistry, 2013, 288, 34190-34204.	1.6	48
65	Timeâ€Dependent Diaryl Ether Inhibitors of InhA: Structure–Activity Relationship Studies of Enzyme Inhibition, Antibacterial Activity, and in vivo Efficacy. ChemMedChem, 2014, 9, 776-791.	1.6	48
66	Infrared spectroscopy reveals multi-step multi-timescale photoactivation in the photoconvertible protein archetype dronpa. Nature Chemistry, 2018, 10, 845-852.	6.6	48
67	Determination of [ <sup>11</sup> C]Rifampin Pharmacokinetics within Mycobacterium tuberculosis-Infected Mice by Using Dynamic Positron Emission Tomography Bioimaging. Antimicrobial Agents and Chemotherapy, 2015, 59, 5768-5774.	1.4	47
68	Evaluating the Contribution of Transition-State Destabilization to Changes in the Residence Time of Triazole-Based InhA Inhibitors. Journal of the American Chemical Society, 2017, 139, 3417-3429.	6.6	46
69	Evidence for electrophilic catalysis in the 4-chlorobenzoyl-CoA dehalogenase reaction: UV, Raman, and 13C-NMR spectral studies of dehalogenase complexes of benzoyl-CoA adducts. Biochemistry, 1995, 34, 13881-13888.	1.2	45
70	Raman Study of the Polarizing Forces Promoting Catalysis in 4-Chlorobenzoate-CoA Dehalogenaseâ€. Biochemistry, 1997, 36, 10192-10199.	1.2	45
71	Development of Modern InhA Inhibitors to Combat Drug Resistant Strains of Mycobacterium tuberculosis. Current Topics in Medicinal Chemistry, 2007, 7, 489-498.	1.0	42
72	Slow Onset Inhibition of Bacterial β-Ketoacyl-acyl Carrier Protein Synthases by Thiolactomycin. Journal of Biological Chemistry, 2010, 285, 6161-6169.	1.6	42

#	Article	IF	CITATIONS
73	Ultrafast Dynamics of Protein Proton Transfer on Short Hydrogen Bond Potential Energy Surfaces: S65T/H148D GFP Journal of the American Chemical Society, 2010, 132, 1452-1453.	6.6	42
74	FTIR studies of hydrogen bonding between α,β-unsaturated esters and alcohols. Journal of Molecular Structure, 1996, 379, 135-142.	1.8	41
75	BLUF Domain Function Does Not Require a Metastable Radical Intermediate State. Journal of the American Chemical Society, 2014, 136, 4605-4615.	6.6	41
76	CoA Adducts of 4-Oxo-4-phenylbut-2-enoates: Inhibitors of MenB from the <i>M. tuberculosis</i> Menaquinone Biosynthesis Pathway. ACS Medicinal Chemistry Letters, 2011, 2, 818-823.	1.3	40
77	Structure of Hexadienoyl-CoA Bound to Enoyl-CoA Hydratase Determined by Transferred Nuclear Overhauser Effect Measurements:Â Mechanistic Predictions Based on the X-ray Structure of 4-(Chlorobenzoyl)-CoA Dehalogenaseâ€. Biochemistry, 1997, 36, 2211-2220.	1.2	39
78	Asparagine deprivation mediated by <i>Salmonella</i> asparaginase causes suppression of activation-induced T cell metabolic reprogramming. Journal of Leukocyte Biology, 2016, 99, 387-398.	1.5	39
79	Resonance Raman and Fourier transform infrared spectroscopic studies of the acyl carbonyl group in [3-(5-methyl-2-thienyl)acryloyl]chymotrypsin: evidence for artifacts in the spectra obtained by both techniques. Biochemistry, 1991, 30, 4790-4795.	1.2	38
80	Photoactivation of the BLUF Protein PixD Probed by the Site-Specific Incorporation of Fluorotyrosine Residues. Journal of the American Chemical Society, 2017, 139, 14638-14648.	6.6	38
81	Ultrafast Infrared Spectroscopy of an Isotope-Labeled Photoactivatable Flavoprotein. Biochemistry, 2011, 50, 1321-1328.	1.2	36
82	Femtosecond to Millisecond Dynamics of Light Induced Allostery in the <i>Avena sativa</i> LOV Domain. Journal of Physical Chemistry B, 2017, 121, 1010-1019.	1.2	36
83	A Virtual Screen Discovers Novel, Fragment-Sized Inhibitors of <i>Mycobacterium tuberculosis</i> InhA. Journal of Chemical Information and Modeling, 2015, 55, 645-659.	2.5	35
84	Substrate Recognition by $\hat{l}^2$ -Ketoacyl-ACP Synthases. Biochemistry, 2011, 50, 10678-10686.	1.2	34
85	Critical role of reverse transcriptase in the inhibitory mechanism of CNI-H0294 on HIV-1 nuclear translocation Proceedings of the National Academy of Sciences of the United States of America, 1996, 93, 11859-11864.	3.3	33
86	Excited State Structure and Dynamics of the Neutral and Anionic Flavin Radical Revealed by Ultrafast Transient Mid-IR to Visible Spectroscopy. Journal of Physical Chemistry B, 2012, 116, 5810-5818.	1.2	33
87	Vibrationally Resolved Photoabsorption Spectroscopy of Red Fluorescent Protein Chromophore Anions. Physical Review Letters, 2003, 90, 118103.	2.9	32
88	Insight through Molecular Mechanics Poissonâ^'Boltzmann Surface Area Calculations into the Binding Affinity of Triclosan and Three Analogues for FabI, the E. coli Enoyl Reductase. Journal of Medicinal Chemistry, 2006, 49, 4574-4580.	2.9	32
89	Thiolactomycin-based β-Ketoacyl-AcpM Synthase A (KasA) Inhibitors. Journal of Biological Chemistry, 2013, 288, 6045-6052.	1.6	32
90	Pharmacokinetic–pharmacodynamic models that incorporate drug–target binding kinetics. Current Opinion in Chemical Biology, 2019, 50, 120-127.	2.8	31

#	Article	IF	CITATIONS
91	Discovery of a cofactor-independent inhibitor of <i>Mycobacterium tuberculosis</i> InhA. Life Science Alliance, 2018, 1, e201800025.	1.3	31
92	Inhibiting enoyl-ACP reductase (FabI) across pathogenic microorganisms by linear sesquiterpene lactones from Anthemis auriculata. Phytomedicine, 2008, 15, 1125-1129.	2.3	30
93	Potential of Lichen Secondary Metabolites against <i>Plasmodium</i> Liver Stage Parasites with FAS-II as the Potential Target. Journal of Natural Products, 2013, 76, 1064-1070.	1.5	30
94	Rational Modulation of the Induced-Fit Conformational Change for Slow-Onset Inhibition in <i>Mycobacterium tuberculosis</i> InhA. Biochemistry, 2015, 54, 4683-4691.	1.2	30
95	Synthesis of Crotonyl-OxyCoA:Â A Mechanistic Probe of the Reaction Catalyzed by Enoyl-CoA Hydratase. Journal of the American Chemical Society, 2001, 123, 506-507.	6.6	29
96	Involvement of Glycine 141 in Substrate Activation by Enoyl-CoA Hydrataseâ€. Biochemistry, 2001, 40, 1725-1733.	1.2	29
97	Substituted diphenyl ethers as a broad-spectrum platform for the development of chemotherapeutics for the treatment of tularaemia. Journal of Antimicrobial Chemotherapy, 2009, 64, 1052-1061.	1.3	29
98	Mechanism and Inhibition of the FabV Enoyl-ACP Reductase from <i>Burkholderia mallei</i> . Biochemistry, 2010, 49, 1281-1289.	1.2	29
99	Structural and Functional Studies of Fatty Acyl Adenylate Ligases from E. coli and L. pneumophila. Journal of Molecular Biology, 2011, 406, 313-324.	2.0	29
100	Mechanism and inhibition of the Fabl enoyl-ACP reductase from Burkholderia pseudomallei. Journal of Antimicrobial Chemotherapy, 2011, 66, 564-573.	1.3	29
101	Unraveling the Mechanism of a LOV Domain Optogenetic Sensor: A Glutamine Lever Induces Unfolding of the Jα Helix. ACS Chemical Biology, 2020, 15, 2752-2765.	1.6	29
102	Stereoselectivity of Enoyl-CoA Hydratase Results from Preferential Activation of One of Two Bound Substrate Conformers. Chemistry and Biology, 2002, 9, 1247-1255.	6.2	28
103	Gas-phase absorption properties of DsRed model chromophores. Physical Chemistry Chemical Physics, 2003, 5, 3021-3026.	1.3	28
104	Characterizing septum inhibition in Mycobacterium tuberculosis for novel drug discovery. Tuberculosis, 2008, 88, 420-429.	0.8	28
105	Thiolactomycin-Based Inhibitors of Bacterial β-Ketoacyl-ACP Synthases with in Vivo Activity. Journal of Medicinal Chemistry, 2016, 59, 5377-5390.	2.9	28
106	Direct observation of the titration of substrate carbonyl groups in the active site of .alphachymotrypsin by resonance Raman spectroscopy. Biochemistry, 1989, 28, 6701-6709.	1.2	27
107	Active Site Heterogeneity in Dimethyl Sulfoxide Reductase fromRhodobacter capsulatusRevealed by Raman Spectroscopyâ€. Biochemistry, 2001, 40, 440-448.	1.2	27
108	An Ordered Water Channel in <i>Staphylococcus aureus</i> FabI: Unraveling the Mechanism of Substrate Recognition and Reduction. Biochemistry, 2015, 54, 1943-1955.	1.2	27

#	Article	IF	CITATIONS
109	Mechanism of MenE Inhibition by Acyl-Adenylate Analogues and Discovery of Novel Antibacterial Agents. Biochemistry, 2015, 54, 6514-6524.	1.2	27
110	A quantitative mechanistic PK/PD model directly connects Btk target engagement and in vivo efficacy. Chemical Science, 2017, 8, 3434-3443.	3.7	27
111	Mechanism of the AppA <sub>BLUF</sub> Photocycle Probed by Site-Specific Incorporation of Fluorotyrosine Residues: Effect of the Y21 p <i>K</i> <sub>a</sub> on the Forward and Reverse Ground-State Reactions. Journal of the American Chemical Society, 2016, 138, 926-935.	6.6	26
112	Antibacterial Activity and Mode of Action of a Sulfonamide-Based Class of Oxaborole Leucyl-tRNA-Synthetase Inhibitors. ACS Infectious Diseases, 2019, 5, 1231-1238.	1.8	26
113	Quantifying the Interactions between Biomolecules: Guidelines for Assay Design and Data Analysis. ACS Infectious Diseases, 2019, 5, 796-808.	1.8	26
114	Medium-Chain Acyl-Coenzyme A Dehydrogenase Bound to a Product Analogue, Hexadienoyl-Coenzyme A: Effects on Reduction Potential, pKa, and Polarizationâ€. Biochemistry, 2000, 39, 13982-13992.	1.2	25
115	Ultrafast Structural Dynamics of BlsA, a Photoreceptor from the Pathogenic Bacterium <i>Acinetobacter baumannii</i> . Journal of Physical Chemistry Letters, 2014, 5, 220-224.	2.1	25
116	Stereospecificity of the Reaction Catalyzed by Enoyl-CoA Hydratase. Journal of the American Chemical Society, 2000, 122, 3987-3994.	6.6	24
117	Correlating drug–target kinetics and in vivo pharmacodynamics: long residence time inhibitors of the Fabl enoyl-ACP reductase. Chemical Science, 2016, 7, 5945-5954.	3.7	24
118	Antitubercular activity of 1,2,3-triazolyl fatty acid derivatives. European Journal of Medicinal Chemistry, 2017, 125, 842-852.	2.6	24
119	Protein Photochromism Observed by Ultrafast Vibrational Spectroscopy. Journal of Physical Chemistry B, 2013, 117, 11954-11959.	1.2	23
120	Complete Proton Transfer Cycle in GFP and Its T203V and S205V Mutants. Angewandte Chemie - International Edition, 2015, 54, 9303-9307.	7.2	23
121	A Methyl 4-Oxo-4-phenylbut-2-enoate with in Vivo Activity against MRSA That Inhibits MenB in the Bacterial Menaquinone Biosynthesis Pathway. ACS Infectious Diseases, 2016, 2, 329-340.	1.8	22
122	Functional dynamics of a single tryptophan residue in a BLUF protein revealed by fluorescence spectroscopy. Scientific Reports, 2020, 10, 2061.	1.6	22
123	Molecular structures of cis- and trans-S-Ethyl thiocrotonate. A combined vibrational spectroscopic and ab initio SCF-MO study. Journal of the Chemical Society, Faraday Transactions, 1994, 90, 3491.	1.7	21
124	Localized electron polarization in a substrate analog binding to the active site of enoyl-CoA hydratase: Raman spectroscopic and conformational analyses of rotamers of hexadienoyl thiolesters. Biospectroscopy, 1995, 1, 387-394.	0.4	21
125	Ultrafast transient mid IR to visible spectroscopy of fully reduced flavins. Physical Chemistry Chemical Physics, 2011, 13, 17642.	1.3	21
126	Vibrational Assignment of the Ultrafast Infrared Spectrum of the Photoactivatable Flavoprotein AppA. Journal of Physical Chemistry B, 2012, 116, 10722-10729.	1.2	21

#	Article	IF	CITATIONS
127	The Francisella tularensis Fabl Enoyl-Acyl Carrier Protein Reductase Gene Is Essential to Bacterial Viability and Is Expressed during Infection. Journal of Bacteriology, 2013, 195, 351-358.	1.0	21
128	Markedly different acyl papain structures deacylate at similar rates: resonance Raman spectroscopic and kinetic evidence. Journal of the American Chemical Society, 1991, 113, 4297-4303.	6.6	20
129	4-Hydroxycinnamoyl-CoA:  An Ionizable Probe of the Active Site of the Medium Chain Acyl-CoA Dehydrogenase. Biochemistry, 2000, 39, 92-101.	1.2	20
130	Variation in LOV Photoreceptor Activation Dynamics Probed by Time-Resolved Infrared Spectroscopy. Biochemistry, 2018, 57, 620-630.	1.2	20
131	Structure–kinetic relationships that control the residence time of drug–target complexes: insights from molecular structure and dynamics. Current Opinion in Chemical Biology, 2018, 44, 101-109.	2.8	20
132	Photophysics of the Blue Light Using Flavin Domain. Accounts of Chemical Research, 2022, 55, 402-414.	7.6	19
133	Chemistry of enzyme–substrate complexes revealed by resonance Raman spectroscopy. Chemical Society Reviews, 1990, 19, 293-316.	18.7	18
134	Time-Resolved Emission Spectra of Green Fluorescent Protein. Photochemistry and Photobiology, 2006, 82, 373.	1.3	18
135	Synthesis of 4-phenoxybenzamide adenine dinucleotide as NAD analogue with inhibitory activity against enoyl-ACP reductase (InhA) of Mycobacterium tuberculosis. Bioorganic and Medicinal Chemistry Letters, 2007, 17, 4588-4591.	1.0	18
136	Structure of the Yersinia pestis FabV Enoyl-ACP Reductase and Its Interaction with Two 2-Pyridone Inhibitors. Structure, 2012, 20, 89-100.	1.6	18
137	Fatty Acid Biosynthesis and Oxidation. , 2010, , 231-275.		17
138	Elucidation of the Protonation States of the Catalytic Residues in <i>mt</i> KasA: Implications for Inhibitor Design. Biochemistry, 2011, 50, 5743-5756.	1.2	17
139	Site-Specific Protein Dynamics Probed by Ultrafast Infrared Spectroscopy of a Noncanonical Amino Acid. Journal of Physical Chemistry B, 2019, 123, 9592-9597.	1.2	17
140	Crystal Structure and Raman Studies of dsFP483, a Cyan Fluorescent Protein from Discosoma striata. Journal of Molecular Biology, 2008, 378, 871-886.	2.0	16
141	A Novel Interaction Linking the FAS-II and Phthiocerol Dimycocerosate (PDIM) Biosynthetic Pathways. Journal of Biological Chemistry, 2008, 283, 31719-31725.	1.6	16
142	Correlating Drug–Target Residence Time and Post-antibiotic Effect: Insight into Target Vulnerability. ACS Infectious Diseases, 2020, 6, 629-636.	1.8	16
143	The biodistribution of 5-[18F]fluoropyrazinamide in Mycobacterium tuberculosis-infected mice determined by positron emission tomography. PLoS ONE, 2017, 12, e0170871.	1.1	16
144	Probing mechanisms of resistance to the tuberculosis drug isoniazid: Conformational changes caused by inhibition of InhA, the enoyl reductase fromMycobacterium tuberculosis. Protein Science, 2007, 16, 1617-1627.	3.1	15

#	Article	IF	CITATIONS
145	Ultrafast electronic and vibrational dynamics of stabilized A state mutants of the green fluorescent protein (GFP): Snipping the proton wire. Chemical Physics, 2008, 350, 193-200.	0.9	15
146	Effect of Mutagenesis on the Stereochemistry of Enoyl-CoA Hydrataseâ€. Biochemistry, 2002, 41, 12883-12890.	1.2	14
147	Substituted Diphenyl Ethers as a Novel Chemotherapeutic Platform against Burkholderia pseudomallei. Antimicrobial Agents and Chemotherapy, 2014, 58, 1646-1651.	1.4	14
148	The Burkholderia pseudomallei Enoyl-Acyl Carrier Protein Reductase Fabl1 Is Essential for <i>In Vivo</i> Growth and Is the Target of a Novel Chemotherapeutic with Efficacy. Antimicrobial Agents and Chemotherapy, 2014, 58, 931-935.	1.4	14
149	Femtosecond stimulated Raman study of the photoactive flavoprotein AppABLUF. Chemical Physics Letters, 2017, 683, 365-369.	1.2	14
150	Positron Emission Tomography Imaging of <i>Staphylococcus aureus</i> Infection Using a Nitro-Prodrug Analogue of 2-[ <sup>18</sup> F]F- <i>p</i> Aminobenzoic Acid. ACS Infectious Diseases, 2020, 6, 2249-2259.	1.8	14
151	Structural Basis for the Regulation of Biofilm Formation and Iron Uptake in <i>A. baumannii</i> by the Blue-Light-Using Photoreceptor, BlsA. ACS Infectious Diseases, 2020, 6, 2592-2603.	1.8	14
152	Substrate Recognition by the Human Fatty-acid Synthase. Journal of Biological Chemistry, 2005, 280, 42612-42618.	1.6	13
153	A Raman-active competitive inhibitor of OMP decarboxylase. Bioorganic Chemistry, 2006, 34, 59-65.	2.0	13
154	Electron transfer quenching in light adapted and mutant forms of the AppA BLUF domain. Faraday Discussions, 2015, 177, 293-311.	1.6	13
155	Computer-aided identification, synthesis, and biological evaluation of novel inhibitors for botulinum neurotoxin serotype A. Bioorganic and Medicinal Chemistry, 2015, 23, 5489-5495.	1.4	13
156	Stereoselective Synthesis, Docking, and Biological Evaluation of Difluoroindanediol-Based MenE Inhibitors as Antibiotics. Organic Letters, 2016, 18, 6384-6387.	2.4	13
157	Structure/Function of Medium Chain Acyl-CoA Dehydrogenase: The Importance of Substrate Polarization. Archives of Biochemistry and Biophysics, 1999, 370, 16-21.	1.4	12
158	Identification of the vibrational marker of tyrosine cation radical using ultrafast transient infrared spectroscopy of flavoprotein systems. Photochemical and Photobiological Sciences, 2021, 20, 369-378.	1.6	12
159	Probing Hydrogen-Bonding Interactions in the Active Site of Medium-Chain Acyl-CoA Dehydrogenase Using Raman Spectroscopyâ€. Biochemistry, 2003, 42, 11846-11856.	1.2	11
160	Procatalytic Ligand Strain. Ionization and Perturbation of 8-Nitroxanthine at the Urate Oxidase Active Site. Biochemistry, 2005, 44, 11440-11446.	1.2	11
161	Evidence from Raman Spectroscopy That InhA, the Mycobacterial Enoyl Reductase, Modulates the Conformation of the NADH Cofactor to Promote Catalysis. Journal of the American Chemical Society, 2007, 129, 6425-6431.	6.6	11
162	CNS Anticancer Drug Discovery and Development: 2016 conference insights. CNS Oncology, 2017, 6, 167-177.	1.2	10

#	Article	IF	CITATIONS
163	Vibrational spectroscopy of flavoproteins. Methods in Enzymology, 2019, 620, 189-214.	0.4	10
164	Excited State Vibrations of Isotopically Labeled FMN Free and Bound to a Light–Oxygen–Voltage (LOV) Protein. Journal of Physical Chemistry B, 2020, 124, 7152-7165.	1.2	10
165	Excited State Resonance Raman of Flavin Mononucleotide: Comparison of Theory and Experiment. Journal of Physical Chemistry A, 2021, 125, 6171-6179.	1.1	10
166	Characterization of trans- and cis-5-methylthienylacryloyl chymotrypsin using Raman difference spectroscopy, NMR, and kinetics: carbonyl environment and reactivity. Journal of the American Chemical Society, 1993, 115, 8757-8762.	6.6	9
167	Deacylation and Reacylation for a Series of Acyl Cysteine Proteases, Including Acyl Groups Derived from Novel Chromophoric Substratesâ€. Biochemistry, 1996, 35, 12487-12494.	1.2	9
168	Stereospecific1H and13C NMR Assignments of Crotonyl CoA and Hexadienoyl CoA:Â Conformational Analysis and Comparison with Proteinâ~CoA Complexes. Journal of the American Chemical Society, 1998, 120, 9988-9994.	6.6	9
169	Radiolabelling and positron emission tomography of PT70, a time-dependent inhibitor of InhA, the Mycobacterium tuberculosis enoyl-ACP reductase. Bioorganic and Medicinal Chemistry Letters, 2015, 25, 4782-4786.	1.0	9
170	Diacyltransferase Activity and Chain Length Specificity ofMycobacterium tuberculosisPapA5 in the Synthesis of Alkyl β-Diol Lipids. Biochemistry, 2015, 54, 5457-5468.	1.2	9
171	Rotational Isomerism in CH3CH2C(:S)SR (R = CH3, CH2CH3): a Combined Vibrational Spectroscopic and ab Initio Study. The Journal of Physical Chemistry, 1994, 98, 3592-3600.	2.9	8
172	A quick method for purifying bile salt-activated lipases. Biotechnology Letters, 1996, 10, 523.	0.5	8
173	Another brick in the wall. , 2000, 7, 94-96.		8
174	Radiosynthesis and biological evaluation of a novel enoyl-ACP reductase inhibitor for Staphylococcus aureus. European Journal of Medicinal Chemistry, 2014, 88, 66-73.	2.6	8
175	A [32P]NAD+-based method to identify and quantitate long residence time enoyl-acyl carrier protein reductase inhibitors. Analytical Biochemistry, 2015, 474, 40-49.	1.1	8
176	Exploring the chemical space of 1,2,3-triazolyl triclosan analogs for discovery of new antileishmanial chemotherapeutic agents. RSC Medicinal Chemistry, 2021, 12, 120-128.	1.7	7
177	Resonance Raman and absorption spectroscopic characterization of the chemically engineered enzyme thiolsubtilisin; comparison with a natural thiolenzyme. Journal of Molecular Liquids, 1989, 42, 195-212.	2.3	6
178	Striking changes observed in key acyl-enzyme linkages by resonance Raman experiments near 77 K. Journal of the American Chemical Society, 1989, 111, 1496-1497.	6.6	6
179	Selectivity of Pyridone- and Diphenyl Ether-Based Inhibitors for the <i>Yersinia pestis</i> FabV Enoyl-ACP Reductase. Biochemistry, 2016, 55, 2992-3006.	1.2	6
180	Rationalizing the Binding Kinetics for the Inhibition of the <i>Burkholderia pseudomallei</i> FabI1 Enoyl-ACP Reductase. Biochemistry, 2017, 56, 1865-1878.	1.2	5

#	Article	IF	CITATIONS
181	Impact of Target Turnover on the Translation of Drug-Target Residence Time to Time-Dependent Antibacterial Activity. ACS Infectious Diseases, 2021, 7, 2755-2763.	1.8	5
182	Observation of carbonyl stretch vibrations in acyl-chymotrypsins by using Fourier transform infrared spectroscopy. Biochemical Society Transactions, 1985, 13, 929-930.	1.6	4
183	Rotational isomerism in CH3C(î—»S)î—,SCH3 and CH3C(î—»S)î—,Sî—,CH2CH3: a combined vibrational spectrosco ab initio study. Journal of Molecular Structure, 1994, 323, 59-69.	pic and 1.8	4
184	Personalized Combined Organic Spectroscopy Problems—Online and in the Lab. Journal of Chemical Education, 2001, 78, 1208.	1.1	4
185	Ultrafast proton transfer in the green fluorescent protein: Analysing the instantaneous emission at product state wavelengths. Journal of Photochemistry and Photobiology A: Chemistry, 2012, 234, 21-26.	2.0	4
186	Formulation studies of InhA inhibitors and combination therapy to improve efficacy against Mycobacterium tuberculosis. Tuberculosis, 2016, 101, 8-14.	0.8	4
187	Structure-Based Design, Synthesis, and Biological Evaluation of Non-Acyl Sulfamate Inhibitors of the Adenylate-Forming Enzyme MenE. Biochemistry, 2019, 58, 1918-1930.	1.2	4
188	A Long Residence Time Enoyl-Reductase Inhibitor Explores an Extended Binding Region with Isoenzyme-Dependent Tautomer Adaptation and Differential Substrate-Binding Loop Closure. ACS Infectious Diseases, 2021, 7, 746-758.	1.8	4
189	Molecular structure of S-ethylthioacrylate Combined vibrational spectroscopic and ab initioSCF-MO study. Journal of the Chemical Society, Faraday Transactions, 1997, 93, 3619-3624.	1.7	3
190	The Catalytic Mechanism of MenB, the 1,4â€Đihydroxynaphthoyl oA Synthase from Mycobacterium Tuberculosis. FASEB Journal, 2006, 20, A41.	0.2	3
191	Ultraviolet resonance Raman spectroscopy of a highly specific acyl-papain. Biochemical Society Transactions, 1985, 13, 930-931.	1.6	2
192	Multiple forms of thioacetyl coenzyme A binding to citrate synthase. Resonance Raman evidence. Journal of the American Chemical Society, 1992, 114, 8738-8739.	6.6	2
193	DePakeing of Dipolar Chemical-Shift NMR Spectra. Journal of Magnetic Resonance Series A, 1993, 102, 110-113.	1.6	2
194	Rotational isomers of N-(β-phenylpropionyl)alanine ethyl dithioester: a Raman spectroscopic and MO study. Journal of Molecular Structure, 1994, 324, 113-122.	1.8	2
195	Synthesis of chromophoric dipeptides as substrates for papain. Bioorganic and Medicinal Chemistry Letters, 1995, 5, 2381-2384.	1.0	2
196	Ring Current Effects in the Active Site of Medium-Chain Acyl-CoA Dehydrogenase Revealed by NMR Spectroscopy. Journal of the American Chemical Society, 2005, 127, 8424-8432.	6.6	2
197	CHAPTER 4. Narrow Spectrum Antibacterial Agents. RSC Drug Discovery Series, 0, , 76-102.	0.2	2
198	Radical Formation in the Photoactivated Adenylate Cyclase OaPAC Revealed by Ultrafast Spectroscopy. Biophysical Journal, 2020, 118, 608a.	0.2	1

#	Article	IF	CITATIONS
199	N/C Terminal Relocation, Truncation, and Native Chemical Ligation; Accessing the Chromophore of Green Fluorescent Protein. FASEB Journal, 2006, 20, A965.	0.2	1
200	Ultrafast Photoreactions in the Green Fluorescent Protein Studied Through Time Resolved Vibrational Spectroscopy. Springer Series in Chemical Physics, 2007, , 468-470.	0.2	1
201	Ultrafast Protein Dynamics Probed by Site Specific Transient IR Spectroscopy. , 2020, , .		1
202	Time resolution of events in an enzyme's active site at 4 K and 300 K using resonance Raman spectroscopy. , 1991, , .		0
203	Resonance Raman spectroscopic and kinetic consequences of a nitrogen sulphur enzyme-substrate contact in a series of dithioacylpapains. Biophysical Journal, 1992, 63, 191-196.	0.2	Ο
204	FACILE CHARACTERIZATION OF THE SPECTRA OF cis AND trans PHOTOISOMERS IN A MIXTURE OF ACYL-ENZYMES BY RAMAN DIFFERENCE SPECTROSCOPY. Photochemistry and Photobiology, 1994, 60, 432-434.	1.3	0
205	Protein Protocols on CD-ROM. John M. Walker. Quarterly Review of Biology, 1999, 74, 70-71.	0.0	Ο
206	Noninvasive Determination of 2-[ <sup>18</sup> F]-Fluoroisonicotinic Acid Hydrazide Pharmacokinetics by Positron Emission Tomography in Mycobacterium tuberculosis-Infected Mice. Antimicrobial Agents and Chemotherapy, 2013, 57, 678-678.	1.4	0
207	Transient IR study of Blue Light Sensing Proteins. EPJ Web of Conferences, 2013, 41, 07009.	0.1	Ο
208	Editorial overview: Next generation therapeutics. Current Opinion in Chemical Biology, 2018, 44, A1-A4.	2.8	0
209	Ultrafast Photoreactions in the Green Fluorescent Protein Studied Through Time Resolved Vibrational Spectroscopy. , 2006, , .		Ο
210	Comparative Structural and Biochemical Studies of Chorismate Binding Enzymes, MenF, EntC and Mbtl. FASEB Journal, 2006, 20, A463.	0.2	0
211	The Kinetic Studies of saFabI, the Enoyl ACP Reductase From Staphylococcus aureus. FASEB Journal, 2007, 21, A999.	0.2	0
212	Targeting the Enoylâ€Reductase Enzyme (FabI): Modern Drug Discovery Effects to Combat Tularemia. FASEB Journal, 2008, 22, 791.6.	0.2	0
213	Investigation of Menaquinone Biosynthesis in Mycobacterium Tuberculosis : Catalytic Mechanism and Inhibition Studies of MenB. FASEB Journal, 2008, 22, 611.15.	0.2	0
214	Ultrafast dynamics of the BLUF mutant dAppA Q63E revealed by TRIR and fluorescent upconversion. , 2010, , .		0
215	Ultrafast Proton Transfer in Fluorescent and Photochromic Proteins. , 2010, , .		0
216	Mechanism and Inhibition of the Dihydroxynaphthoyl 0A Synthase MenB from Mycobacterium Tuberculosis. FASEB Journal, 2010, 24, 463.11.	0.2	0

#	Article	IF	CITATIONS
217	Imaging the Distribution of Carbonâ€11 Labeled Rifampicin, Isoniazid and Pyrazinamide in Baboons using PET. FASEB Journal, 2010, 24, 907.7.	0.2	0
218	Residence Time and in vivo Antibacterial Activity ―A Critical Aspect of Lead Compound Optimization. FASEB Journal, 2010, 24, 680.3.	0.2	0
219	Slow Onset Inhibitors of Bacterial Fatty Acid Biosynthesis: Residence Time, In Vivo Activity and In Vivo Imaging. FASEB Journal, 2010, 24, 71.3.	0.2	Ο
220	Featured Article Editorial. ACS Infectious Diseases, 2020, 6, 3089-3089.	1.8	0